# FREIE UNIVERSITÄT BERLIN
## FORTGESCHRITTENENPRAKTIKUM PHYSIK

## Report on the Construction of the PM2-Beamline at BESSY II

*Author:*
Michael Goerz

*Supervisor:*
Dr. Ralph Püttner

15. November 2007

# Contents

**Summary**

This report describes the construction work that Anton Haase and I did on the PM2 beamline at BESSY II between April and July 2007. We found the beamline in a semi-constructed condition and were able to bring it to an almost operational status. The details of our work are described in Section 4.

Before that, I will give some background information on synchrotron radiation and BESSY II in general in Sections 1- 2, followed by a review of the theoretical basics in Section 3. The report concludes with a documentation of the beamline's current status in Section 5. There is an appendix describing the control electronics for the monochromator.

# 1   Introduction
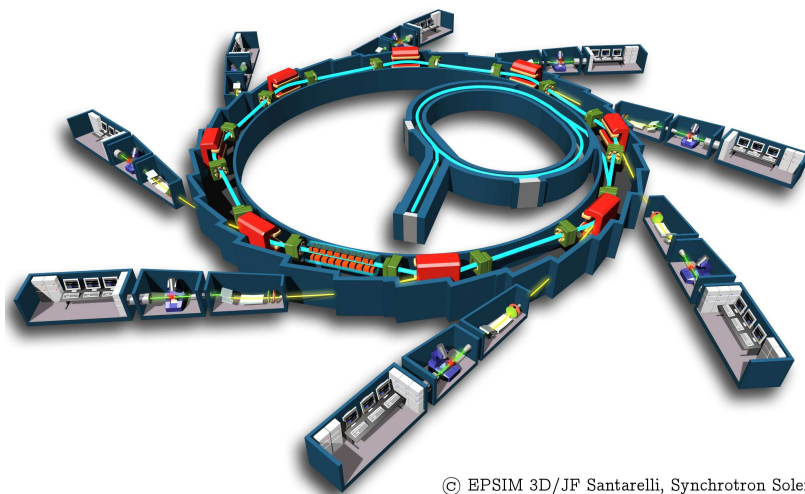


© EPSIM 3D/JF Santarelli, Synchrotron Soleil

Fig. 1: General Schematic of a Synchrotron

In broad areas of physics and engineering, there is need for a source of electromagnetic radiation, e.g. for scattering experiments, excitation of electronic states, microscopy, and a huge number of other applications. Traditional light sources, such as X-ray tubes or simple discharge lamps, are rather limited in their intensity, spectrum, continuity, and brilliance. Additionally, researchers wish for a light source that can be used over a broad spectrum instead of just specific wavelengths (e.g. lines of an X-ray tube).

These requirements can be fulfilled by synchrotron radiation. A synchrotron is a specific type of particle accelerator, in which electrons are kept in circulation at ultra-relativistic speeds – i.e. effectively at the speed of light – by carefully placed strong magnets. Due to the well known phenomenon of the emission of electromagnatic radiation by charged particles undergoing acceleration, these accelerated electrons can be used as a source for a wide variety of light from the visible part up to the hard X-ray part of the spectrum: the necessary acceleration is produced by the bending magnets keeping the electrons in their path.

Additionally, there are specialized *insertion devices*, undulators and wigglers, which produce alternative and variable radiation characteristics.

## 1.1  Historic Overview



Fig. 2: Aerial View of BESSY II

BESSY II is a synchrotron of the third generation and has been in operation since 1998. It replaced the second generation BESSY I (1982-1999), which had been the first dedicated source of synchrotron radiation in Germany.

Synchrotron radiation was first observed in 1947 by John Blewett at the General Electrics Research Lab in Schenectady , New York[1], even though there had been theoretical work much earlier. Since the observation was in a specific type of particle accelerator in which bunches of electrons travel in a circle with a fixed radius – a synchrotron, that also became the name stuck to the radiation.

Initially, synchrotron radiation was a major nuissance for the particle accelerators, since it causes the particles to lose energy as they are forced on their circular path. It took some years until the scientific potential of the effect was recognized. The first experimental use of synchrotron radiation for spectroscopy was not until about 10 years later (in 1956). First research programs appeared in the 1960s.

At first, researchers had to use the radiation that occurred as "waste" in existing particle accelerators. These were the synchrotrons of the first generation. With increased need, the first dedicated accelerators were built, with the specific purpose of generating synchrotron radiation for experimental needs. In these second generation facilities, the radiation produced at the bending magnets was forwarded into beamlines. Finally, more specialized and effective devices (undulators and wigglers) for the generation of synchrotron radiation were developed. The modern third generation synchrotrons such as BESSY II have long straight sections where these devices are put in place, in addition to the traditional bending magnets. Recently, there is some development towards forth generation devices, most notably the *free electron laser*, which is also currently in planning at the BESSY II site.

---

[1] See [6] and [15] for an introduction on the historic origins.

## 1.2 Properties of Synchrotron Radiation

Synchrotron radiation has some properties that make it uniquely suitable for scientific purposes:

- broad spectrum

- high brilliance and great focusing conditions

- high intensity

- polarization

- pulsed

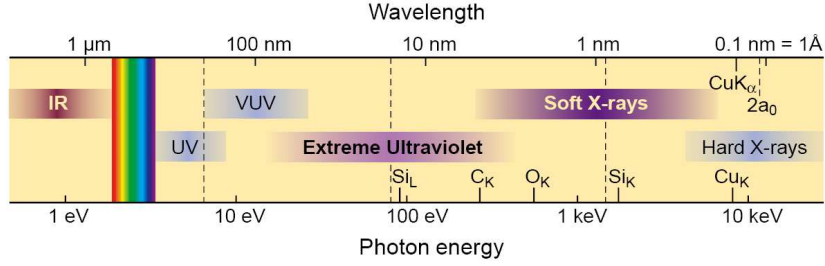- highly predictable and controllable

- vacuum conditions



Fig. 3: The Electro-Magnetic Spectrum, from [4]

The first notable property is the wide spectrum that synchrotron radiation encompasses. It includes the full range shown in Fig. 3, from the low infrared through visible light up to the hard X-rays, and may even extend into somewhat lower and higher energies. It includes the primary resonance energies of all elements.
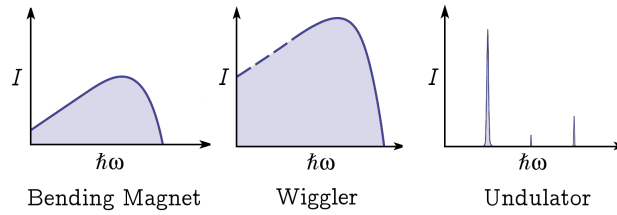


Fig. 4: Spectrum characteristics for Bending Magnets, Wigglers, and Undulators

The specific spectrum characteristics depend on the insertion device[2], as shown in Fig. 4. Bending magnets and wigglers generate a broad frequency

---

[2]I also count the bending magnets as insertion devices. Some people differentiate between bending magnets and undulators/wigglers, referring only to the latter two as insertion devices.

distribution, undulators have sharp peaks. The insertion devices can be adapted for each beamline, and there will be variable monochromators built in to achieve great flexibility.

In all cases, the beam of synchrotron radiation is highly collimated, as is often expressed by the *brilliance*, one of the most characteristic measures of quality:

$$B \quad = \quad \frac{N_f}{0.1\%, \text{mm}^2 \text{mrad}^2} \tag{1}$$

The brilliance is defined as the number of photons per second ($N_f$) per 0.1% bandwidth per area per solid angle.[3] For experimental purposes, the high brilliance translates into a high intensity of the synchrotron light.

Due to the design of the insertion devices, the synchrotron radiation has linear or elliptical polarization. Also, since the electrons travel in very localized bunches[4], the radiation that the experimentalist sees is pulsed. At BESSY II, the frequency is 500 MHz, with each pulse lasting 0.02 ns.

The theory of synchrotron radiation (see Section 3) is very well understood and allows very precise calculation of the radiation characteristics. The insertion devices can be manufactured and adapted with equal precision, so that for each experiment, the conditions are highly controllable. It is this precision and flexibility – each beamline can receive the exact desired radiation due to the use of insertion devices – that separates third generation synchrotrons from earlier setups.

Lastly, the entire synchrotron operation including the beamlines has to take place in an ultra-high-vacuum environment; maintaining an electron beam would be impossible otherwise. This has the added benefit that researchers do not have to worry about their samples becoming contaminated in an atmosphere.

## 1.3  Applications

There is a wide variety of research from different fields of science and engineering taking place at BESSY II, which illustrates the importance of synchrotron light sources.

The original report proposing the construction of BESSY II [1] already takes 50 pages to explicate the intended uses in eight different categories.

In atomic and molecular physics, the broad spectrum is suitable for a detailed spectroscopy of energy levels, among many other things. The high intensity is needed to work with low-density (non-solid-state) samples.

In chemistry, a number of processes can be examined, such as photochemical processes, in which the light is used to manipulate chemical bondings, dynamic processes that need rapid pulse and highly intense radiation, and spectroscopy of clusters (systems of few atoms).

Listed next is matrix isolation spectroscopy, in which atomic structures (atoms, molecules, clusters) are insterted at low temperatures into a host grid, which isolates and stabilizes them, allowing detailed chemical analysis.

---

[3] See [8]. This quantity is sometimes also called *spectral brightness*. It is also sometimes expressed at power per bandwith, area, and solid angle (See [3]). For a comment on the ambiguity of nomenclature, see [13].

[4]This is due to the workings of the accelerator, which will be explained in Section 2.

In solid state physics, the spectroscopy with photo-absorption and -emission requires a tunable light source. There is a research group at BESSY II working within the solid state field on magnetic nano-structures.

For the physics of surfaces and interfaces, most of the spectroscopic methods used in solid state physics can also be used in a surface sensitive mode. However, a high intensity of radiation is needed, as well as the spacial and spectral resolution that the synchrotron can provide.

Another important field is X-ray microscopy. The resolution of optical microscopes is limited by the wavelength of the used light, so that short wavelength X-rays can provide a major improvement. This method has some benefits to alternatives such as electron microscopy, which places severe restrictions on the samples.

The Physikalisch-Technische-Bundesanstalt (PTB) uses BESSY II for various tasks of radiometry. They define standards of measurement, as well as test and calibrate industrial products. Because the synchrotron light source is so controllable, it can serve as a standard.

Lastly, there are several other industrial applications, most notably in the microengineering field. The Anwenderzentrum für Mikrotechnik (AZM) uses the excellent light characteristics for X-ray lithography for the engineering of nano-structures.

All of these tasks, among some others, are currently being worked on at BESSY II. The BESSY website[5] and the "Highlights" brochure [9] inform about current research activities. Most notable beyond the ones mentioned above are the installation of an infra-red beamline, which is used for the spectroscopy of biological samples as well as some other purposes. There is also a lot of activity at the development of new generation synchrotrons. The insertion devices are in constant development, and as a long term project, the free electron laser [2] is planned as an addition to the facility.

The breathtaking multitude of all the projects, which I can only list here without much explanation, shows how important synchrotron radiation is as a tool of scientific research.

## 2    Operations at BESSY II

We can now look in some detail at how synchrotron radiation is produced and delivered at the beamlines. Fig. 5 shows a detailed map of the facility, including all beamlines[6]. We will follow the steps 1-8 as they are labeled in the figure. A brief outline of the electron beam generation and acceleration appears in [12].

### 2.1    Electron Generation

At step (1), electrons are generated from a simple filament in a vacuum tube, and are first accelerated by the anode voltage in the tube. They then enter a *racetrack microtron*, which works as shown in Fig. 6. The microtron is a simple but effective device, in which the electron beam is passed through a linear accelerator (red tube) repeatedly. After each pass, the beam is turned

---

[5]http://www.bessy.de
[6]You may also go back to Fig. 1 for comparison, it depicts the same basic synchrotron structure, leaving out wigglers and undulators

Fig. 5: Detailed Map of Ring Structure and Beamlines at BESSY II

180° by a magnetic field (green). As the electrons' kinetic energy increases, they spiral outwards, but still go through the accelerator each cycle. Finally, when they have reached their maximum energy, 50 MeV, they leave the microtron.
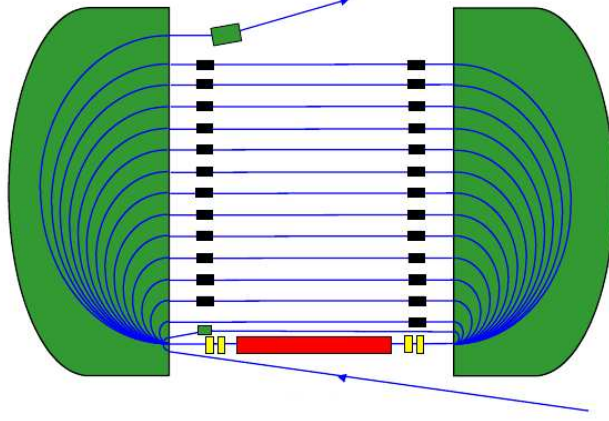


Fig. 6: Racetrack Microtron, from [16]

## 2.2 The Synchrotron Ring

So far, we have referred to the entire BESSY II or similar facilities as "synchrotron". This is common usage, but not entirely correct. The term synchrotron does in fact refer to a specific circular type of *accelerator*, which is the next step (2) in the processing of the electron beam. The synchrotron is only the smaller inner circle of 96 m circumference, whereas the large outer circle with 240 m circumference to which the beamlines are connected is properly called the *storage ring*.

In the synchrotron ring, the electrons are accelerated to their final energy of 1.7 GeV (max. 1.9 GeV). The acceleration happens through cavity resonators (see Section 2.6), and the electrons are kept in their circular paths by regular bending magnets.

The bending magnets are simple dipole magnets, similar to the storage ring dipole magnets shown in Fig. 7. They have a homogeneous magnetic field, so that the electron is forced on a circular path with radius

$$r = \frac{v \cdot \gamma \cdot m_e}{e \cdot B}. \tag{2}$$

As the speed of the electrons increases and approaches the speed of light, the magnets have to adapt with an increased magnetic field. This is what separates the synchrotron ring from the storage ring. The synchrotron ring is purely an accelerator, which is used only for brief periods, whereas in the storage ring, the electrons are kept at a constant speed for an extended period of time (several hours). The beamlines rely on the constant energy of the electron beam in the storage ring.
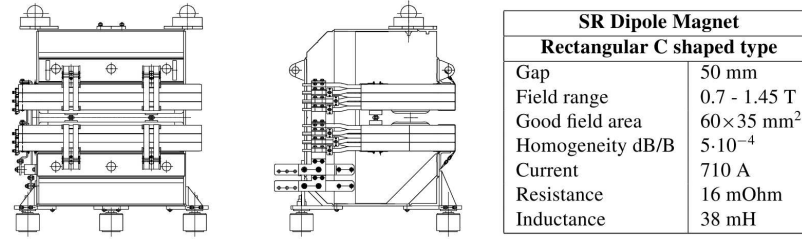
| SR Dipole Magnet | |
|---|---|
| Rectangular C shaped type | |
| Gap | 50 mm |
| Field range | 0.7 - 1.45 T |
| Good field area | $60{\times}35$ mm$^2$ |
| Homogeneity dB/B | $5{\cdot}10^{-4}$ |
| Current | 710 A |
| Resistance | 16 mOhm |
| Inductance | 38 mH |

Fig. 7: Storage Ring Dipole Magnets, from [5]

## 2.3 Injection

When the electron beam has reached its final velocity, it is injected into the storage ring at step (3). For this purpose, a carefully timed *kicker* magnet deflects the electron beam out of the synchrotron ring into the injection line, with another kicker pushing it into the storage ring.
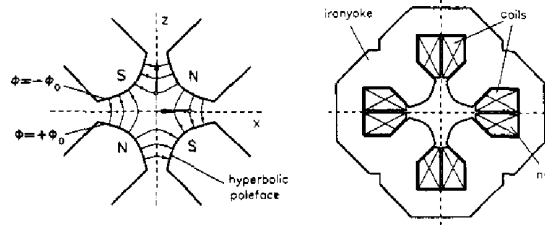
## 2.4 Focusing



Fig. 8: Sketch of a Quadrupole Bending Magnet, from [18]

Once in the storage ring, the electron beam is kept in circulation for up to ten hours. To keep the beam stable during this time, and to compensate for aberrations caused by the dipole magnets and other insertion devices, it is important to keep the electron beam focused. This is done with multipole magnets. The different magnetic devices and their parameters are available in [5, 7].

The simplest layout, a quadrupole magnet, is shown in Fig. 8. It is easy to see that the electron beam is pushed back to the center (perpendicular to the magnetic field lines) if it deviates from the center.

Other multipole magnets are used in a similar vein; they can have more specialized properties such as the compensation of chromatic errors.

A magnetic focusing element is labeled as step (4) in Fig. 5

## 2.5 Insertion Devices

In order to extract the synchrotron radiation from the storage ring, insertion devices (IDs) are used. This can be bending magnets (5), undulators (6), or
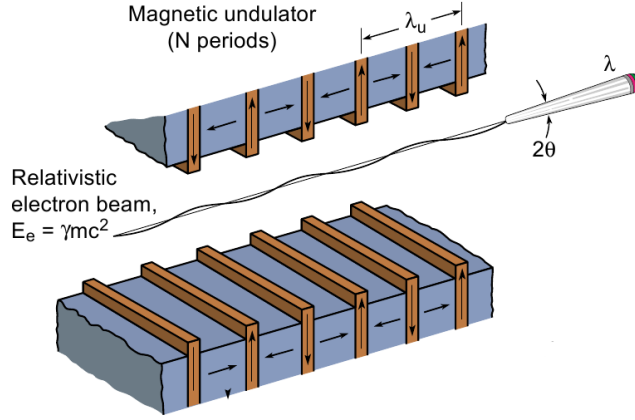
Fig. 9: Schematic of and Undulator/Wiggler, from [4]

wigglers (7). Additionally, there are some wavelength shifters in use at BESSY II. Each ID has different radiation characteristics, as discussed in Section 1.2.

Undulators and wigglers are very similar in their setup. They both use an array of magnets to oscillate the electron beam in a sine-wave (or on an elliptical path for a more complicated variation). As the electrons are accelerated during this process, they emit synchrotron radiation. The principal difference between wigglers and undulators is the strength of the magnets, which corresponds to the amplitude of the oscillations. Undulators use magnets that are approximately as strong as the bending magnets in the storage ring, and therefore only produce smaller oscillations. Wigglers use much stronger fields, generated with super-conducting coils. Specifically, the distinction is made according to the *wiggler strength*

$$K \;=\; \frac{e\lambda_u B_0}{2\pi mc^2}. \tag{3}$$

$B_0$ represents the maximum magnetic field, $\lambda_u$ the wavelength of the sine path, as shown in Fig.9. Large values of $K$ describe wigglers, small numbers ($K = 1.5$) describe undulators.

The difference in terms of the radiation characteristics can be seen in Fig. 10. Due to the extreme deflection of the beam in the wiggler case, the synchrotron radiation cones are spread over a larger space and do not overlap significant-ly. This leads to a broad spectrum, similar to bending magnets. However, the intensity is much higher, with the electron beam being wiggled over multiple (sine) cycles. A bending magnet in comparison only emits radiation from the fraction of a cycle (the fraction of the bending magnet length to the full storage ring circumference)

In the undulator case, the deflection is much smaller, and the radiation cones overlap, causing them to interfere. This leads to a peak in the spectrum (the maximum of constructive interference) in addition to a high intensity.

An additional aspect is polarization. In the simplest case, which we discussed, the polarization of the synchrotron radiation is linear. With more complicated undulator and wiggler setups, where the electrons are forced on a spiral, elliptical polarization can also be obtained.
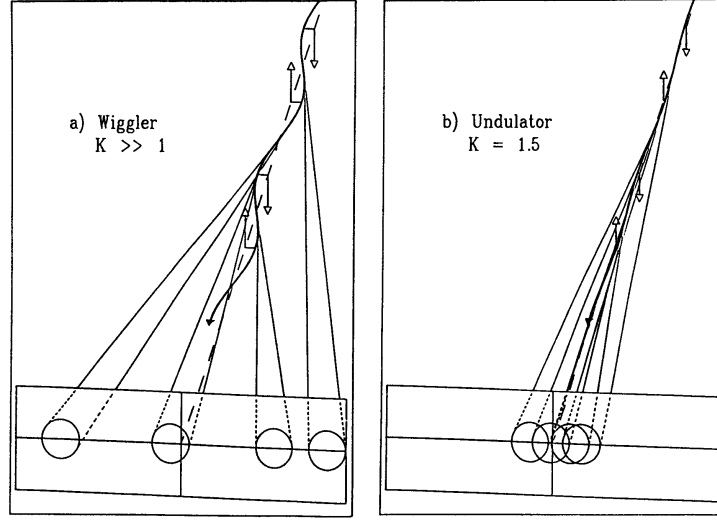
10

Fig. 10: Undulator and Wiggler Radiation, from [1]

The ID in use for the PM2 beamline is a simple dipole bending magnet.
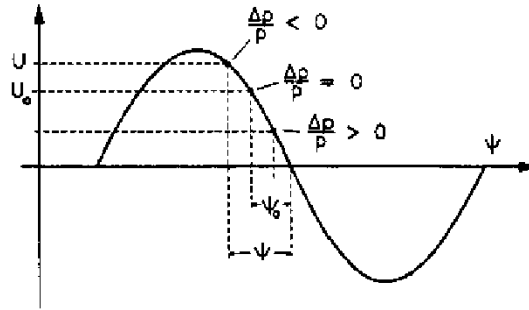
## 2.6 Microwave Cavity Accelerators



Fig. 11: Principle of Microwave Cavity Accelerator, from [18]

Each insertion device extracts energy from the storage ring (the energy of the synchrotron radiation). To compensate for this, the beam has to be accelerated slightly at each cycle to maintain its speed. Additionally, the electrons traveling in a bunch smear out over time and have to be recompressed. Both tasks are fulfilled with a microwave cavity resonator at step (8).

Inside the resonator, there is a standing microwave with a frequency of 500 MHz. As depicted in Fig. 11, the electron beam enters the resonator at a nominal phase $\Psi_0$ of the oscillation, and is accelerated by the energy $e \cdot U_0$. Electrons arriving too late ($\frac{\Delta P}{P} < 0$) see a higher voltage ($U = U(\Psi - \Delta\Psi)$), those arriving too early ($\frac{\Delta P}{P} > 0$) a higher one. In this way, the nominal energy of the electron

beam is enforced, and the loss due to synchrotron radiation is replenished.

Nonetheless, the time the electron beam can be kept stable in the storage ring is limited, at some point the electrons will collide with each other or scatter on the few remaining molecules left in the pipe (imperfections of the vacuum conditions).

## 2.7 Beamlines



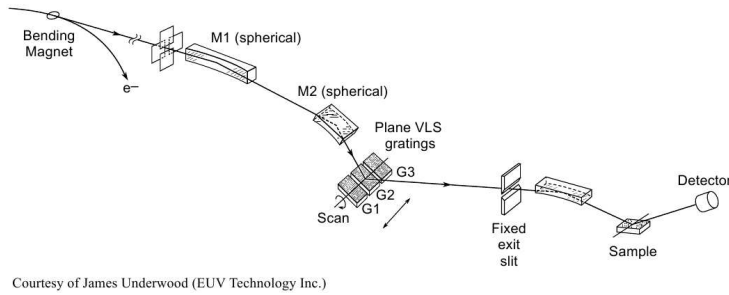Courtesy of James Underwood (EUV Technology Inc.)

Fig. 12: A Typical Beamline, from [4]

Once the synchrotron radiation is generated at the insertion device, the beamline takes the task of adapting the radiation to the experimental needs. This especially means monochromatization and focusing. A typical beamline is shown in Fig. 12.

For bending magnet radiation, all adaptions have to be made within the beamline, while for wigglers and especially for undulators, the parameters (magnetic field, distance between magnetic poles) can be tweaked to produce radiation with the desired characteristics.

Note that for the wavelengths that are typically used, transmission optics such as lenses are no longer feasible. Instead, long curved grazing mirrors are use to focus the beam (M1, M2 in Fig. 12), and adjustable gratings provide the monochromatization.

One of the problems that has to be dealt with for the optics is the heat that is due to the high intensity of the synchrotron radiation. For some beamlines, the optical parts have to be water-cooled.

The workings of the PM2 beamline will be described in more detail in Section 5.

# 3 Theoretical Background

## 3.1 Radiation of Charges in Circular Motion

The theory behind synchrotron radiation is that of a charge moving at relativistic speed. A thorough theoretic discussion of this can be found in [11, Chapter 14]. A comprehensive theoretical overview of all the aspects of the synchrotron operation appears in [18].

The starting point is the radiation of a non-relativistic accelerated charge with its wellknown $\sin^2 \theta$-dependancy. This is the case that is often used to

describe antennas, for example. With $\vec{\beta} = \frac{\vec{v}}{c}$ and $\vec{n}$ being the radial unit vector (pointing in direction of the observer), the power per solid angle is: [7]

$$\frac{\mathrm{d}P}{\mathrm{d}\Omega} = \frac{e^2}{4\pi c}\left|\vec{n} \times (\vec{n} \times \dot{\vec{\beta}})\right|^2 \tag{4}$$

$$= \frac{e^2}{4\pi c^3}|\dot{\vec{v}}|^2 \sin^2\theta \tag{5}$$

In the case of relativistic speed, this formula needs to be adapted. To find the formula describing our case, one has to go back to the Lienard-Wiechert theory of retarded potentials, and look at the radial component of the Poynting vector that comes forth from this analysis:

$$[\vec{S} \cdot \vec{n}]_{\mathrm{ret}} = \frac{e^2}{4\pi c}\left\{\frac{1}{R^2}\left|\frac{\vec{n} \times [(\vec{n} - \vec{\beta}) \times \dot{\vec{\beta}}]}{(1 - \vec{\beta} \cdot \vec{n})^3}\right|^2\right\}_{\mathrm{ret}} \tag{6}$$

$R$ is the distance between the reference point and the position the charge had when it first emitted the radiation that is now visible at the reference point (in the picture of the relativistic light-cone).

From this we get to the power per unit solid angle in the time-frame $t'$ of the electron ($t' = t - R(t')/c$):

$$\frac{\mathrm{d}P(t')}{\mathrm{d}\Omega} = R^2 \vec{S} \cdot \vec{n}\,(1 - \vec{\beta} \cdot \vec{n}) \tag{7}$$

$$= \frac{e^2}{4\pi c}\frac{\left|\vec{n} \times \{(\vec{n} - \vec{\beta}) \times \dot{\vec{\beta}}\}\right|^2}{(1 - \vec{n} \cdot \vec{\beta})^5} \tag{8}$$

Note how Eq. (8) turns into Eq. (4) for $\beta \ll 1$

We can now look at a circular relativistic motion, i.e. $\vec{\beta} \perp \dot{\vec{\beta}}$ and get (with $\Theta$ measured from the direction of $\vec{v}$):

$$\frac{\mathrm{d}P(t')}{\mathrm{d}\Omega} = \frac{e^2}{4\pi c^3}\frac{|\dot{\vec{v}}|^2}{(1 - \beta\cos\Theta)^3}\left[1 - \frac{\sin^2\Theta\cos^2\Phi}{\gamma^2(1 - \beta\cos\Theta)^2}\right] \tag{9}$$

Fig. 13 shows how $\frac{\mathrm{d}P}{\mathrm{d}\Omega}$ develops for increasing relativistic speed. At rest, there is again the classic $\sin^2\theta$ picture. With $\beta = v/c$ going from 0 to 1, the forward pointing lobe inflates massively. The cone pointing backwards at $\beta = 0$ is also pulled in the forward direction (the points of zero emission move from $\pi/2$ to a lower angle). Fig. 14 shows the full radiation cone at a speed of 98% the speed of light, which is not nearly the speed the electrons have in the storage ring. Obviously, the radiation peaks very sharply in the direction of the movement, i.e. in radial direction from the storage ring. It will appear as a "searchlight" whenever the electron beam passes the bending magnet.

There is also a more intuitive explanation to the searchlight property than derivating Eq. (8). The change from a $v = 0$ to $v = c$ can also be understood in terms of the relativistic Doppler effect. For an observer looking at the incoming electron beam, the wavelength is massively shortened. i.e. the energy is massively
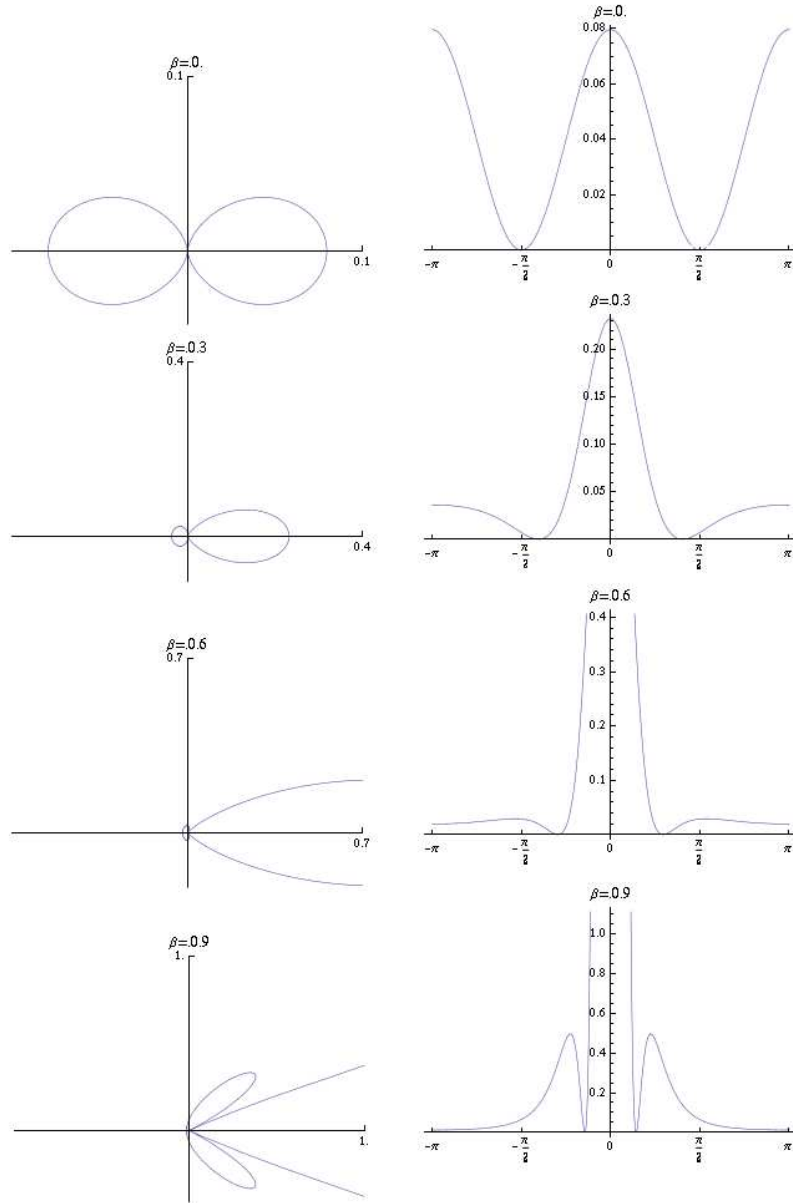
---

[7]cf. [11, p. 665]

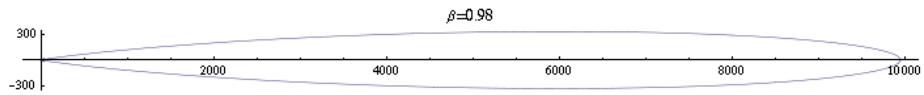Fig. 13: Radiation Cones for Increasing Speeds (arbitrary units)



Fig. 14: Radiation Cone for $v = 0.98c$

14

enlarged. Using the relativistic Doppler effect, it is possible to quantify the narrowness of the cone (i.e. the directedness of the radiation): With the z-Axis pointing in the direction of the movement, and $\vec{k}'$ being the wave vector in the electron's frame of reference and $\vec{k}$ being the wavefactor in the laboratory frame of reference, we can look at $\Theta \approx \frac{k_x}{k_z}$. The Doppler stretching of the wave vector only occurs in z-direction, so $k_x = k'_x$. For $k_z$ we have

$$k_z \quad = \quad \frac{2\pi}{\lambda} \tag{10}$$

$$\lambda \quad = \quad \lambda' \sqrt{\frac{1-\beta}{1+\beta}} \qquad \text{cf. [17]}$$

$$= \quad \lambda' \frac{\sqrt{1-\beta^2}}{1+\beta}$$

$$= \quad \lambda' \frac{1/\gamma}{1+\beta}$$

$$\approx \quad \lambda' \frac{1}{2\gamma} \qquad \text{for } \beta \to 1 \tag{11}$$

$$k_z \quad \approx \quad 2\gamma k'_z \tag{12}$$

This gives us the stretching of a reference angle $\Theta' = \frac{k'_x}{k'_z} = 1$, i.e. the width of the synchrotron radiation:

$$\Theta \approx \frac{k_x}{k_z} \approx \frac{k'_x}{2\gamma k'_z} = \frac{1}{2\gamma} \tag{13}$$

## 3.2  Bending Magnet Radiation

The formulas presented so far describe the general case of accelerated electrons moving in a circle. As such, they directly describe the radiation of bending magnets, but are equally the foundation of the other IDs in which the acceleration is a sine wave. The radiation of charges that are not moving in a circle can be described by applying the above formulas to the (circular) curvature at each point and looking at the superposition of the radiation from all the individual points.

In addition to the directedness and high intensity that Eq. (9) proves for high speeds, Section 1.2 also mentioned the broad spectrum of synchrotron radiation (for bending magnets and wigglers). A good theoretical explanation[8], albeit somewhat handwaving, comes from the use of the Heisenberg uncertainty principle.

$$\Delta E \cdot \Delta \tau \quad \geq \quad \hbar/2 \tag{14}$$

In order to calculate $\Delta E$, we first have to find an expression for $\Delta \tau$, which we can get from looking at Fig. 15. Following the convention usually followed by synchrotron physicists, the half-width of the radiation pulse is $2\Delta\tau$ (Fig. 15(b)). The geometry is presented in Fig. 15(a); with the width of $\theta$ as in Eq. (13), an observer will see radiation while the electrons are between point A and point B,
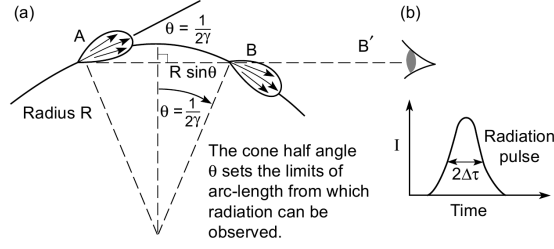
---

[8]following [3]

Fig. 15: Pulse Duration for Bending Magnet Radiation, from [3]

i.e. for the time that the electrons need to travel that distance minus the time the radiation itself needs to travel from A to B. We therefore get

$$
\begin{aligned}
2\Delta\tau &\approx \frac{R \cdot 2\Theta}{v} - \frac{2R\sin\Theta}{c} \\
&\approx \frac{R}{\gamma}\frac{1}{v} = \frac{1}{c}
\end{aligned}
\tag{15}
$$

With Eq. (2) and

$$
(1-\beta) \approx \frac{1}{2\gamma^2}
\tag{16}
$$

we get

$$
2\Delta\tau \approx \frac{m}{2eB\gamma^2}
\tag{17}
$$

and therefore

$$
\Delta E \geq \frac{2e\hbar B\gamma^2}{m}.
\tag{18}
$$

A rather complicated theoretical analysis[9] can provide a formula for the flux of photons of energy $E$ in a given solid angle and bandwidth:

$$
\left.\frac{\mathrm{d}^3 F_B}{\mathrm{d}\Omega\,\mathrm{d}\phi\,\mathrm{d}\omega/\omega}\right|_{\phi=0} = 1.33 \cdot 10^{13} \cdot E_e^2 \cdot I \cdot (\frac{E}{E_c})^2 \cdot K_{2/3}^2\left(\frac{E}{2E_c}\right)
\tag{19}
$$

where $E_e$ is the energy of the electron beam in GeV (1.7 GeV for BESSY II), $I$ is the current in the ring in mA (100 mA), $E_c$ is the critical photon energy – the energy at which half the power is emitted at lower energy and half at higher energy:

$$
E_c = \frac{3e\hbar B\gamma^2}{2m}
\tag{20}
$$

The $K_{2/3}$ are modified Bessel-functions.

---

[9]cf. [10]

16

By integrating over the azimuthal angle $\phi$ on gets a more commonly used expression for the flux that is plotted in Fig. 16 for the parameters of the BESSY ring:[10]

$$\frac{\mathrm{d}^2 F_B}{\mathrm{d}\Omega\,\mathrm{d}\omega/\omega} \quad = \quad 2.46 \cdot 10^{13} \cdot E_e^2 \cdot I \cdot (\frac{E}{E_c})^2 \cdot G\left(\frac{E}{2E_c}\right) \tag{21}$$

with

$$G(x) \quad := \quad x \cdot \int_x^\infty K_{5/3}(x')\,\mathrm{d}x'. \tag{22}$$
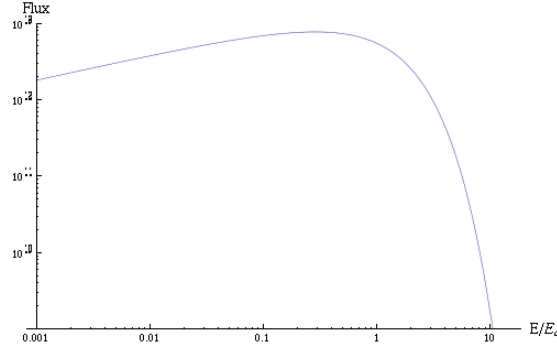


Fig. 16: Flux in photons per second and 0.1% bandwidth for $E_e = 1.7\,\mathrm{GeV}$ and $I = 100$  mA

## 3.3  Undulators and Wigglers

The concept of undulators and wiggles was already explained in Section 2.5. The undulator achieves its characteristic peak in the spectrum due to the constructive interference of the coherent radiation that is thrown off at each oscillation. There are higher modes of that peak, but in almost all cases only the *central cone* is used.

While the formulas for the undulators are important for synchrotrons in general, since the PM2 beamline has a bending magnet as an insertion device, I will not go into as much detail with their derivation.

Most important is the *undulator equation* that calculates the peak wavelength:

$$\lambda \quad = \quad \frac{\lambda_u}{2\gamma^2}\left(1 + \frac{K^2}{2} + \gamma^2\Theta^2\right) \tag{23}$$

with $K$ as defined in Eq. (3) and $\lambda_u$ being the undulator period. The term $\frac{\lambda_u}{2\gamma^2}$ comes out of the relativistic Doppler effect, $\frac{K^2}{2}$ accounts for the transverse motion in the undulator, and $\gamma^2\Theta^2$ is a correction for the radiation off axis.

---

[10]Compare this with `http://www.bessy.de/upload/insertion_devices/files/flux.pdf`

The peak width is described as:

$$\frac{\Delta\lambda}{\lambda} \;=\; \frac{1}{N} \qquad (24)$$

This can be seen when looking at the situation as a Fourier transform: $1/N$ is generally the width of the Fourier transform of $N$ harmonic cycles. In retrospect, the Fourier transform picture also gives an explanation of why the bending magnet spectrum is so broad: the electron in this case only makes a fraction of a cycle (one full cycle is the entire storage ring). In wigglers, contrary to the undulator case, the radiation does not overlap coherently, so there is no peak, but a broad spectrum like for the bending magnets.

We can now look at the opening angle of the cone that would include the bandwidth of Eq. (24). By taking Eq. (23) once off axis ($\Theta \neq 0$) and once on axis ($\Theta = 0$) and dividing the two expressions, one can see that

$$\frac{\Delta\lambda}{\lambda} \;\approx\; \gamma^2\Theta^2 \qquad (25)$$

By demanding that for $\Theta = \Theta_{\mathrm{cent}}$ Eq. (24) holds, we get

$$\Theta_{\mathrm{cen}} \;\approx\; \frac{1}{\gamma\sqrt{N}} \qquad (26)$$

This is the undulator equivalent to Eq. (13).

Finally, the power radiated in the central cone can be calculated as:

$$\bar{P}_{\mathrm{cent}} \;\approx\; \frac{\pi e \gamma^2 I}{\epsilon_0 \lambda_u} \frac{K^2}{(1 + \frac{K^2}{2})^2} \qquad (27)$$

For wigglers, there are no new fundamental new formulas as compared to the bending magnets. The main difference is the higher intensity, and some adjustability of the parameters.

# 4    Description of the Construction Work

The beamline as we found it was complete in its major parts, but was still missing some larger pieces in its second half. The full beamline is shown in Fig. 22, with the parts that we had to add or modify significantly highlighted in red.

The first task was to put in the supporting pillars (Fig. 17). The exact track of the beamline was measured out and marked on the ground by the BESSY staff. Since the beamline has to follow the radiation beam exactly, it is important to have a very precise layout and measurement of the beamline construction. To facilitate this precision, there is a special coordinate system for the entire experimentation hall.

The pillars are screwed to the floor. For this, three holes we drilled for each pillar and filled with a special glue to hold the screw anchor (Fig. 17(a)). This provided an extremely stable and permanent basis for the pillars. The hollow steal pillars were filled with sand for added weight, and then the mounting structure (Fig. 17(b)) had to be assembled on top. The structure is adjustable in height and can rotate horizontally.

(a) Ground Attachment



(b) Mounting Structure

Fig. 17: The Supporting Pillars



(a) Mounted Pipes



(b) Pipe Connection

Fig. 18: Assembly of the Pipes

Next, we put in the two-meter connecting pipes, as shown on Fig. 18. One has to take care to keep the inside of the pipes and all other parts clean, as they will have to provide an ultra-high-vacuum that would be difficult to achieve with significant amounts of dust inside the beamline. Hence all open connectors were covered with plastic (or aluminum foil) caps.

The junction between two pipes, or any two parts in general was done with an abundant number of screws. A copper gasket ring was placed between the two connectors. Copper, as a soft metal, dents under the pressure of the junction and ensures that the construction can hold a vacuum. It takes some practice to make a junction, since the copper rings will not always stay in place easily. Also, special care has to be taken to close all the screws firmly but evenly. Otherwise, leaks may occur.



(a) Assembly of a Pump

(b) Pump with Control Electronics Attachments
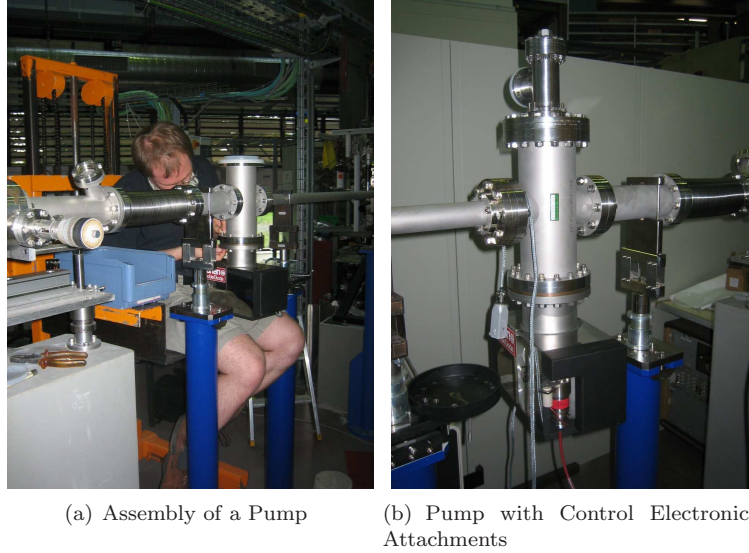
Fig. 19: The Vacuum Pumps

We then added some smaller connecting parts, such as crosses, "bellos" (flexible, accordion-like pieces), sample holders, and windows, and then proceeded to connect several vacuum pumps (Fig. 19. This part of the construction was rather challenging: the pumps are extremely heavy, yet have to be connected hanging, so we used a mechanical lift for putting them into place.

All the pumps that are part of the beamline are *ion-getter-pumps*, which work by ionizing any particles left in the vacuum and pulling them out into the walls with electric fields, where there are chemically bound. For this to work, a vacuum already has to be present. For that, external pumps would be used.

We also added some valves and connected them to the pressurized air system that is provided by BESSY for each beamline. These valves can be controlled electronically, and were connected to the beamline control unit. This also allows for them to be shut automatically when pressure sensors register a drop in the vacuum.

After the large missing parts of the beamline were in place, we spent some time on the refocusing chamber (Fig. 27). The chamber had a number of windows

that needed to be closed, and also, we had to to adjust a set screw that is used to fine-tune the focusing mirror. For this, we had to open the chamber and put in a metal bolt that was specifically manufactured by the fine mechanics lab. As the inside of the chamber was extremely sensitive and not so accessible, and had to be kept as clean as possible, a lot of care was needed.

The next part of our work took place at the pre-monochromator inside the radiation controlled cage, where quick-action stop valve had to be installed.
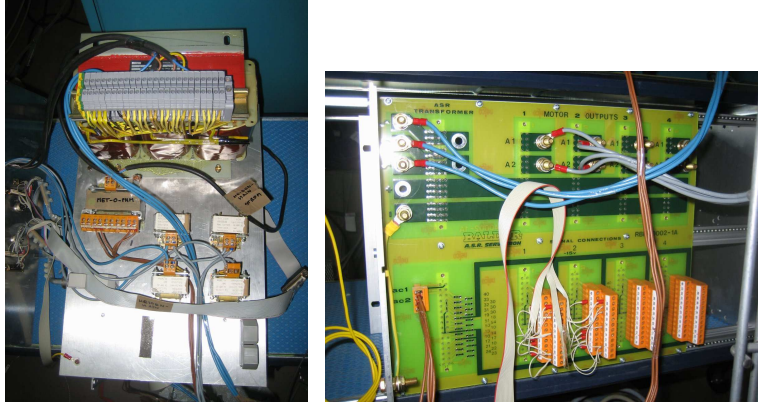


Fig. 20: Control Electronics for the Monochromator

In the last part of the construction work, we organized the control electronics for the monochromator (Fig. 20). The electronics had been stored inactively, we removed them from their old case. Some parts were replaced by the BESSY staff. We then analyzed the layout of the control system by following all connections, with some old documentation, and labeled the different parts. A documentation of the electronic monochromator control system appears in an appendix to this report.

Lastly, after completion of the construction, we connected an external vacuum test pump (turbo-molecular pump) at the ion-getter pump between the pre-monochromator and the monochromator in order to create a vacuum in that part of the beamline (Fig. 21). This had the purpose of testing for leaks in our junctions. After several days, the pump reached fairly low pressure of approx. $10^{-7}$ mbar. As an additional test, we sprayed helium on all the junctions. This is a common test for the integrity of a vacuum: Since the Helium atoms are so small, they would easily infiltrate any leak and could be detected at the pump. The helium test showed no leaks in our construction.

## 5   Layout of the PM2-Beamline

This section will describe the complete layout of the beamline as it was at the end of the work (Fig. 22). The beamline is complete up to the refocusation chamber, anything beyond that (a chamber for the actual sample and detectors) still has to be installed. As discussed previously, the purpose of the beamline is to perform monochromatization and focusing on the synchrotron radiation. Therefore, the main components are two monochromators (the first one for a rough selection,

(a) Vacuum Test Pump        (b) Pump Connection to the Beamline
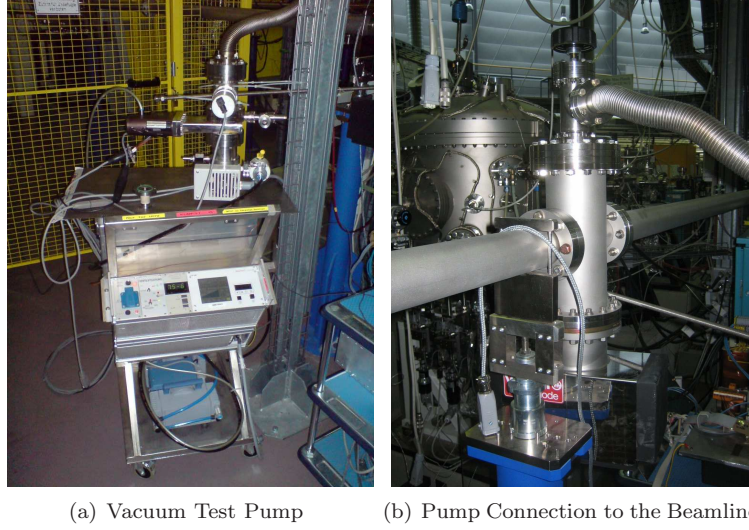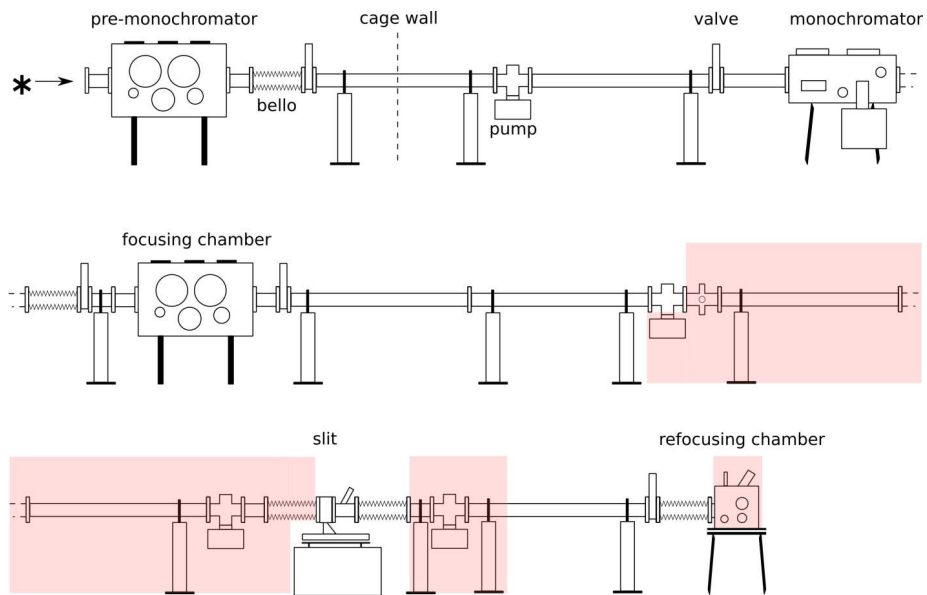
Fig. 21: Testing the Vacuum



Fig. 22: Beamline Layout, the highlighted parts were added by us.

the second one for electronically controlled fine-tuning), a focusing chamber, a slit, and a refocusing chamber. The concept is shown in Fig. 23.
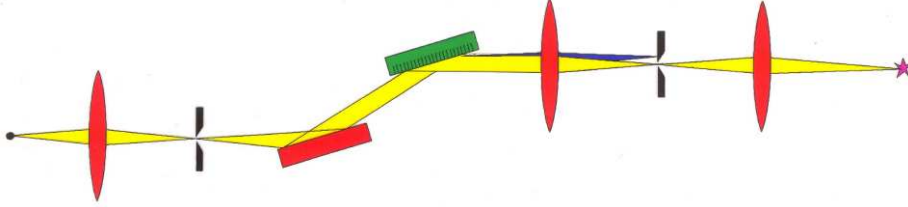


Fig. 23: Beamline Schematic, without pre-monochromator, adapted from [14]

The monochromator unit consists of the planar mirror (red) and the diffraction grating (green), however, the focusing chamber and the slit that follow are integral parts of the monochromatization process. Naively, one would just use a grating to split up the light into different wavelengths, and use a slit to select from the spectrum. However, this is only valid in an ideal model. For a spread-out spectrum, the result would be like shown in Fig. 24 To avoid this
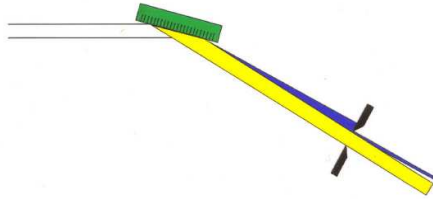


Fig. 24: Imperfect Monochromator, from [14]

deficiency, a lense (mirror) is used and the slit is placed at the focal point, as indicated in Fig. 23

Fig. 25 shows the monochromator, on Fig. 25(b), the grating is visible. The diffractive quality is apparent by the diffraction of the camera flash.

The grating angle can be tuned with control electronics, which are described in the appendix.

The slit is shown in Fig. 26. It is mounted on a sliding rule in order for it to be adaptable to the conditions needed for the experiment. Since different wavelengths have different focal lengths, it is essential to have a movable slit in the monochromating process.

Finally, the refocusing chamber is shown in Fig. 27. On Fig. 27(b), the curved mirror that serves as a lense is visible. The mirrors used earlier in the focusing chamber are in fact significantly larger. The refocusing mirror can be tuned with the set screw that we installed.

The second aspect of the devices installed in the beamline relate to the ultra-high vacuum environment that has to be sustained. This includes the pumps that were discussed in the previous section, and valves. Some of the valves have pressure detectors and will shut automatically when a leak in the beamline is detected. This mechanism serves to protect the expensive main parts, such as the monochromator, from damage due to a lost vacuum and the resulting possible
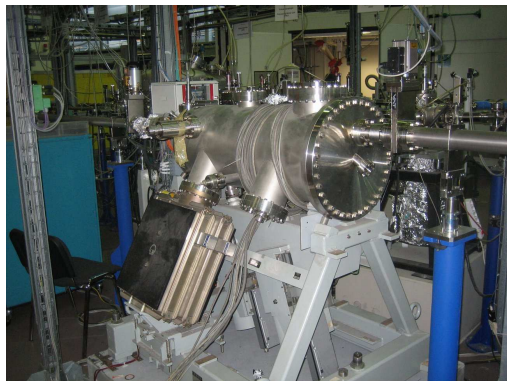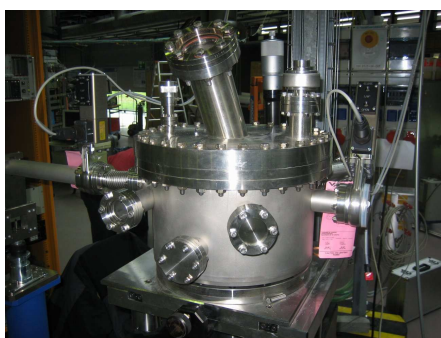
(a) Outside View
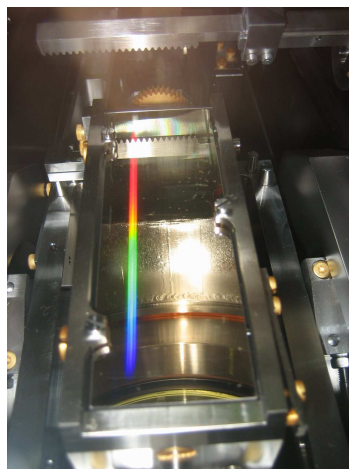
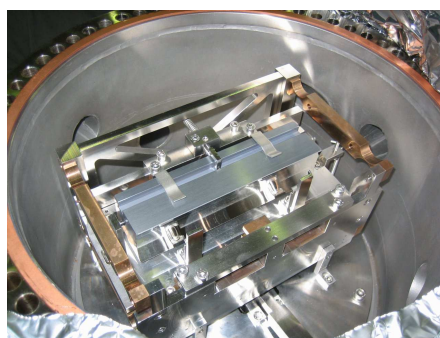

(b) The Grating

Fig. 25: The Monochromator



Fig. 26: Slit



(a) Outside View



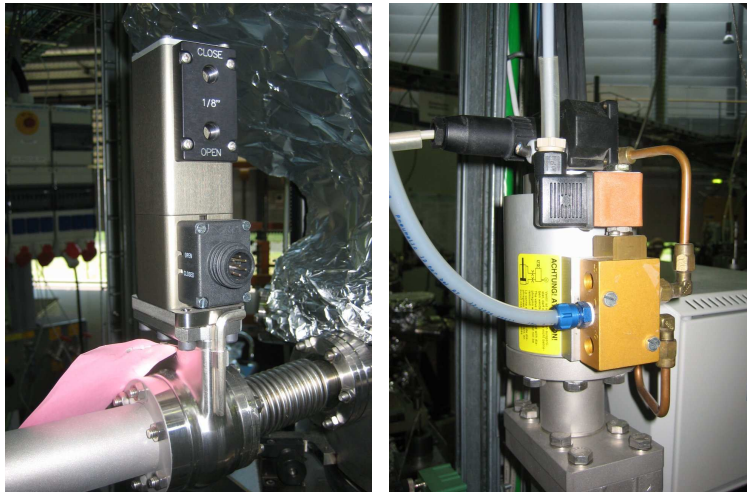(b) Curved Mirror Inside

Fig. 27: The Refocusing Chamber

Fig. 28: Valves

implosion of dust into the beamline. Naturally, they also avoid the worst case of creating a leak of the storage ring, which would immediately disrupt all operations, and take weeks to restore.



Fig. 29: Beamline Control

The valves are connected to an electronic control system shown in Fig. 29, that shows the status of the beamline at all times, and allows different sections to be activated and deactivated. Installing and maintaining these electronics is job of the BESSY staff.
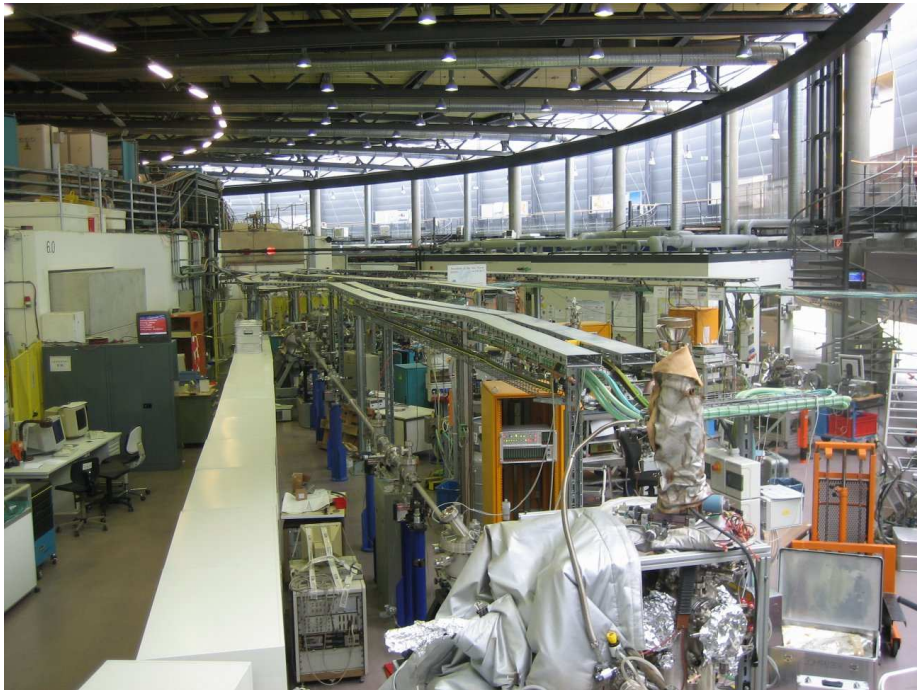
Fig. 30: Overview of the Assembled Beamline

# A    Overview of the Monochromator Control Electronics

This appendix briefly describes the general layout of the electronic control of the monochromator's servo motors, which set the reflection grating and allow to tune the monochromator to the desired wavelength. The details of all the electronics are described in the accompanying manual, however there are some minor differences between the manual and the actual implementation.

The purpose of the entire system is to allow control of the servo motors from a computer, and to manage the power supply. Fig. 35 is a schematic of the entire circuit layout in all its major parts. The two central components are the TSNM boards, one for each motor, which contain the actual control electronics. Each of them receives input from the computer on the pins labeled 10, 24, and 23, and returns signals via pin 12 and 10 to the controlling speedometers (T1, T2), which control the speed of the motors (M1, M2). Also, from the connectors A1 and A2, the TSNM gives power to the motors through limiter coils L1/L2, which prevent power surges. Missing from the schematic is the PSNM board, which regulates the power for both the TSNM's. There is a separate system, the *Heidenhain* system, also not indicated, that monitors the servo motors and provides feedback to the electronics.

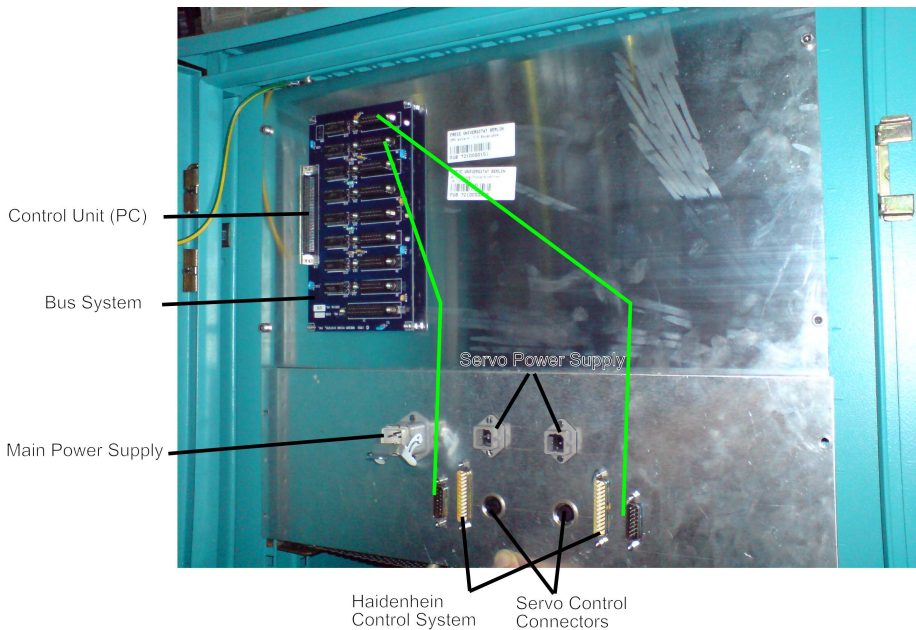Figs. 31 – 35 contain photographs of the system's components in their physical implementation.



Fig. 31: Connection Panel

Fig. 31 shows the front panel of the entire system. From the user's perspective, this panel combines input and output. The computer (which is running an appropriate software) is plugged in at the *Bus System* circuit board. The bus has to be connected to the lower panel, along the bright green lines. The *Main Power*

27

*Supply* is where the entire system receives power. The *Servo Power Supply* and *Servo Control Connectors* constitute the system's output. The power supply has to be connected directly to the motors, in Fig. 35 this missing connection would be the lines between the limiter coils L1/L2 and the motors M1/M2. The *Servo Control Connectors* have to be connected to the controlling speedometers T1/T2, which are physically attached to the motors. This missing connection is the one labeled *Control Circuit* in Fig. 35. The Heidenhain control system is also plugged into this panel.
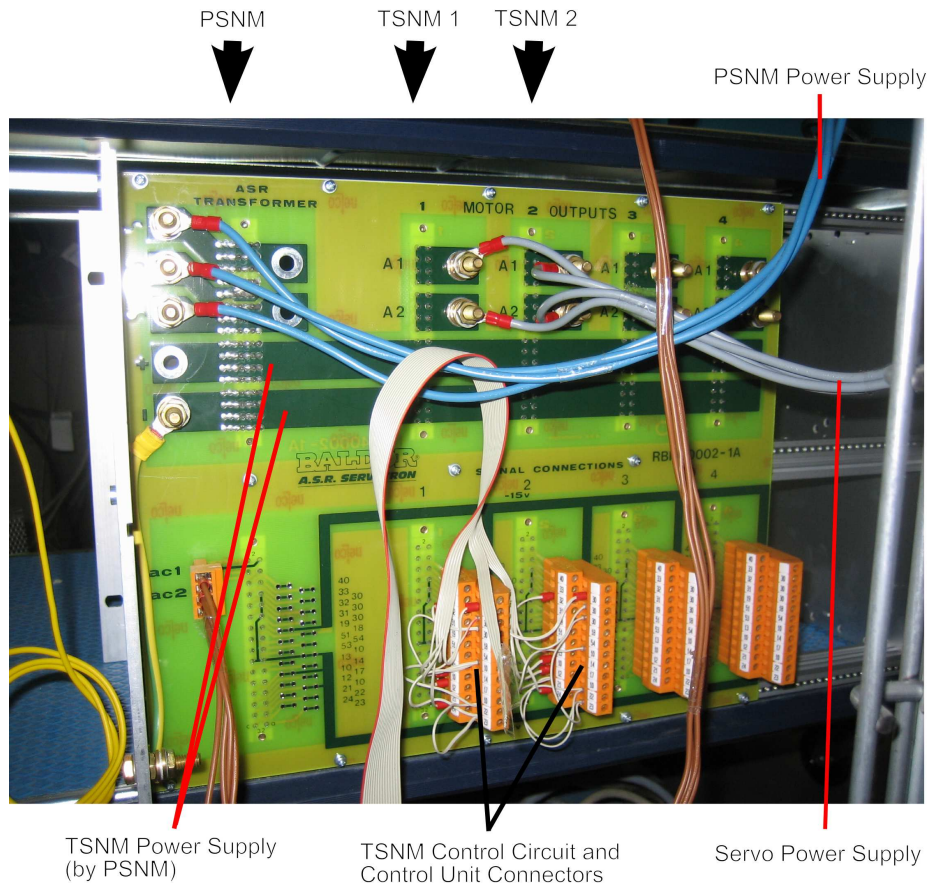


Fig. 32: PSNM/TSNM Board

Fig. 32 shows the system's central component, the PSNM/TSNM board. The PSNM receives power from the three blue cables, which originate from the *Main Power Supply* (Fig. 34). It relays power to the two TSNM's and indirectly to the servo motors (the connection to the servo motors is the gray cables from the A1/A2 connectors of the TSNM's). The power connection between PSNM and TSNM is visible as the two dark green bars on the board. The *TSNM Control Circuit and Control Unit Connector* are in the lower half of the board. The ribbon cable connects to the *Connection Panel* (Fig. 31). In Fig. 35, the ribbon cable would connect between the pins 10-24 of both TSNM's and the T1/T2 speedometers (*Control Circuit*) and the computer (*Control Unit*), respectively.
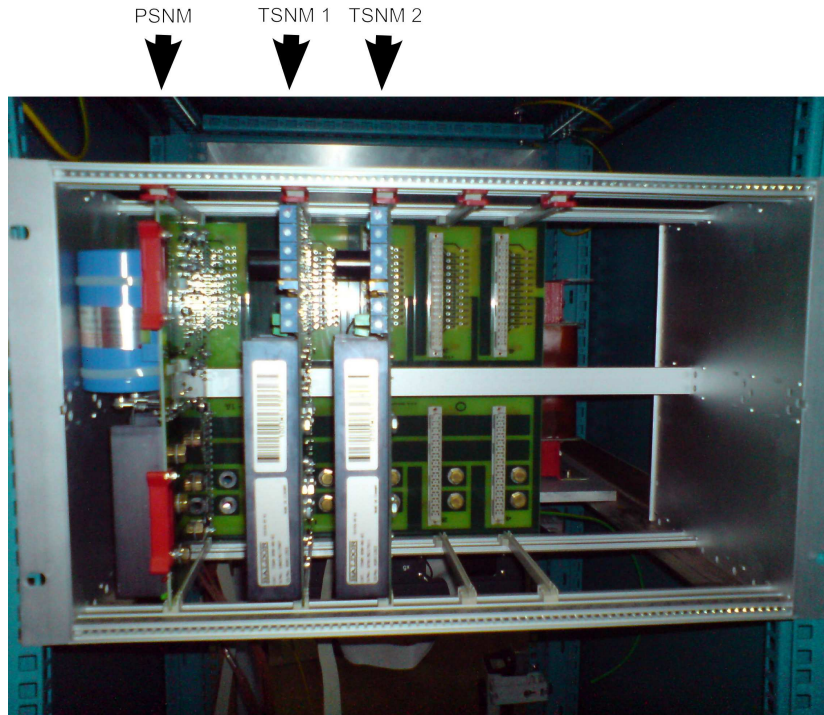
Fig. 33: Frontside of PSNM/TSNM Board

On the side of the *Connection Panel*, the ribbon cable splits up and connects to the four outlets of the *Control Unit* and *Servo Control Connectors* (Fig. 31). The brown cables belong to the Heidenhain system.

Fig. 33 shows the front side of the PSNM/TSNM board. The PSNM and the two TSNM's are plug-in cards.

Fig. 34 shows the intermediate parts between the *Connection Panel* (Fig. 31) and the *PSNM/TSNM Board* (Fig. 32). First, this is the *Main Power Supply* that distributes the power to all components. It draws power from the *Main Power Supply* plug on the *Connection Panel* (Fig. 31) via the black cable at the top. The three bundled blue cables go from the *Main Power Supply* to the PSNM (Fig. 32). Additionally, there is power going to the Heidenhain system, through the device labled as *MET-O-PHM*.

Second, there are the four *Limiter Coils*, which in Fig. 35 are labeled L1/L2. The have the bundled gray cables as input, which originate from the A1/A2 connectors on the TSNM's (Fig. 32), and continue with two gray and two blue cables which go the *Servo Power Supply* on the *Connection Panel* (Fig. 31). The purpose of the coils is simply to limit power surges that would occur when the motors switch on or off.

Fig. 34 also shows the backside of the *Connection Panel* (Fig. 31) on the very left. The splitting-up of the ribbon cable into the *Control Unit* and the *Servo Control Connectors* is visible.
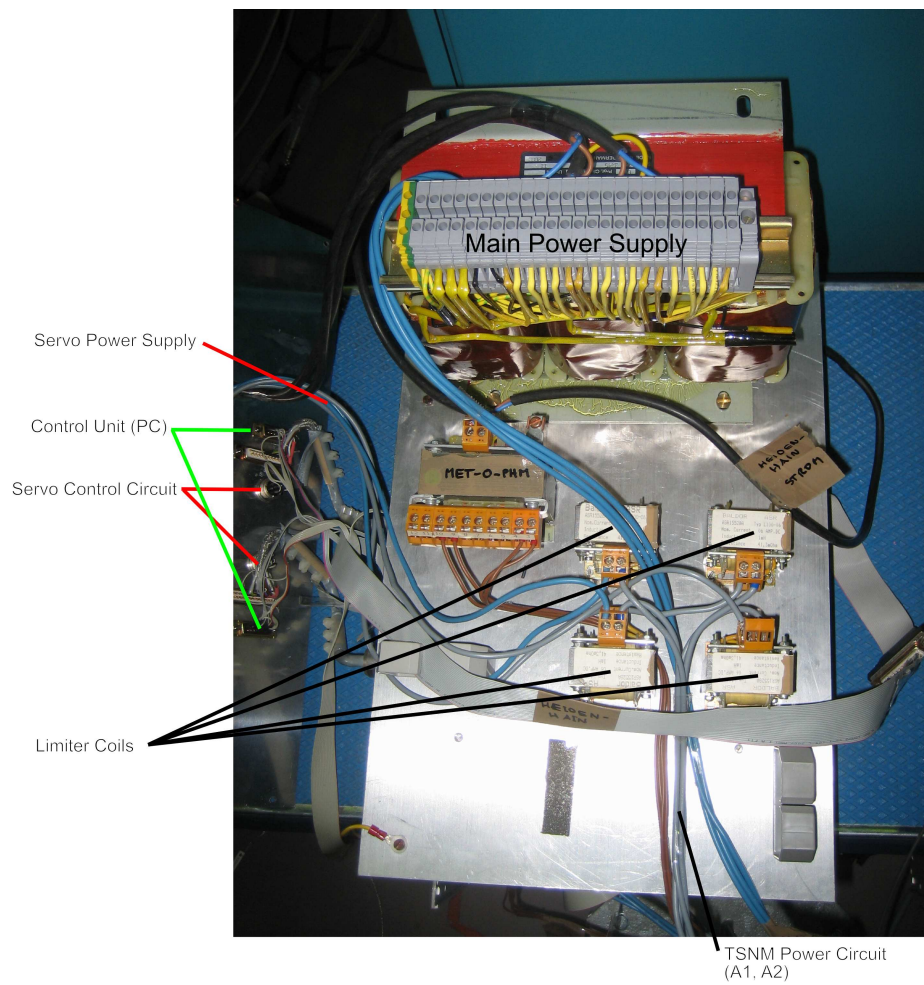
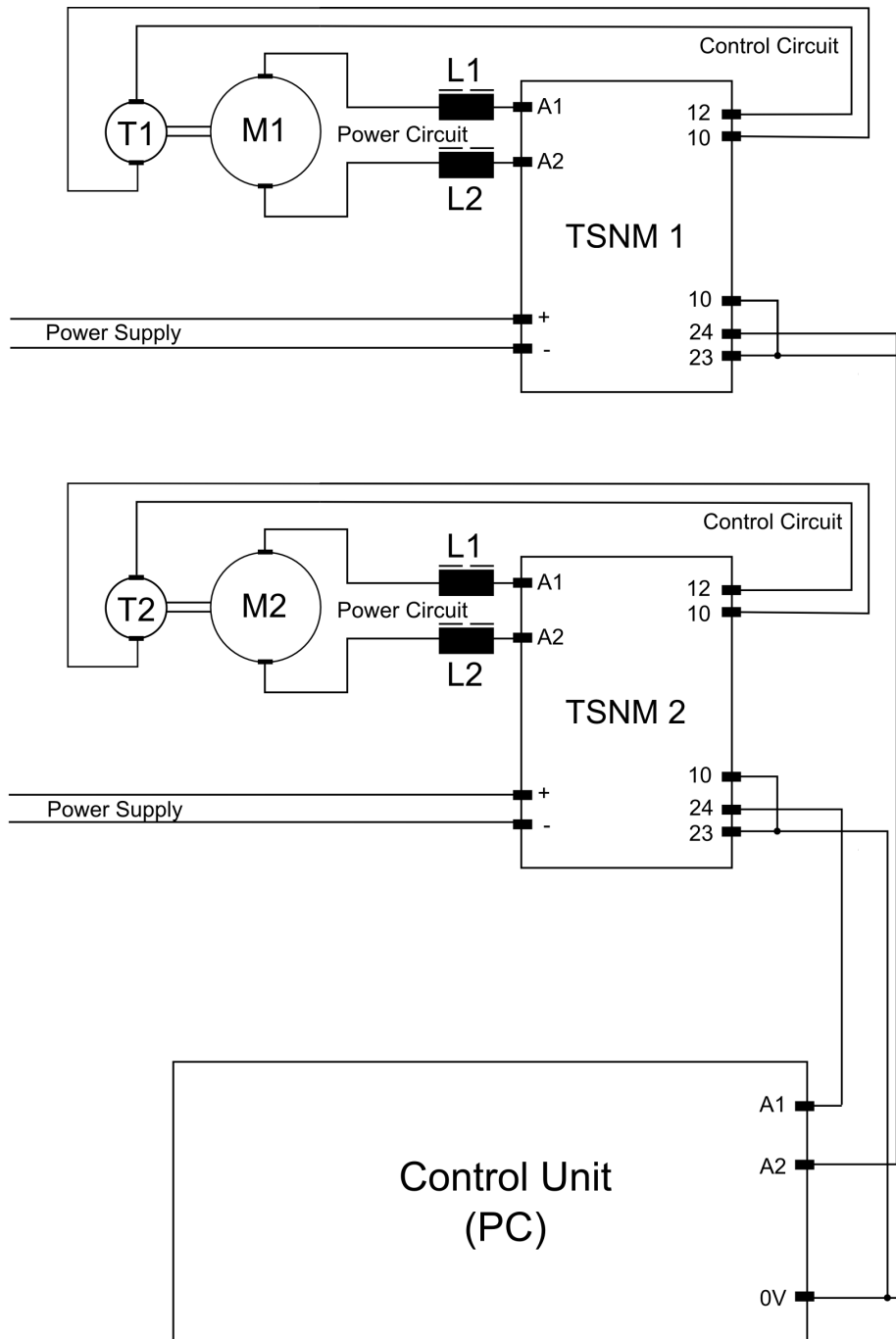Fig. 34: Power Transformer and Limiter Coils

Fig. 35: Circuit Layout of Monochromator Control Electronics

# References

[1] BESSY II – Eine optimierte Undulator/Wiggler-Speicherrung-Lichtquelle für den VUV- und XUV-Spektralbereich / Berliner Elektronenspeicherring-Gesellschaft für Synchrotronstrahlung mbH. Berlin, November 1986 (Vol 1). – Report

[2] BESSY FEL – Technical Design Report / Berliner Elektronenspeicherring-Gesellschaft für Synchrotronstrahlung mbH. URL http://www.bessy.de/cms.php?idcat=94, March 2007. – Report

[3] ATTWOOD, David: *Soft X-Rays and Extreme Ultraviolet Radiation, Principles and Applications*. Cambridge University Press, 2000

[4] ATTWOOD, David: *Synchrotron Radiation for Materials Science Applications – Lecture 1: Introduction to Synchrotron Radiation*. Lecture Slides, UC Berkeley. Spring 2007. – URL http://www.coe.berkeley.edu/AST/srms/

[5] BECKER, T. et.al.: Prototype Developement of the BESSY II Storage Ring Magnetic Elements. In: *Proceedings of the 1993 Particle Accelerator Conference* Vol. 2, 1993, p. 1325–1327

[6] BLEWETT, John P.: Synchrotron Radiation - Early History. In: *J. Synchrotron Rad.* 5 (1998), p. 135–139

[7] BUDZ, P. et.al.: The Magnets of the Metrology Light Source in Berlin-Adlershof. In: *Proceedings of EPAC 2006*, 2006, p. 3296–3298

[8] ERIKSSON, Mikael: Brilliance – an Overview. In: *J. Synchrotron Rad.* 4 (1997), p. 111–113

[9] HENNEKEN, Heike (Ed.) ; SAUERBORN, Markus (Ed.): *Highlights 2006*. Berliner Elektronenspeicherring-Gesellschaft für Synchrotronstrahlung mbH, 2006. – URL http://www.bessy.de/cms.php?idcat=94

[10] HOFMANN, Albert: *The Physics of Synchrotron Radiation*. Cambridge University Press, 2004

[11] JACKSON, John D.: *Classical Electrodynamics*. 3rd Ed. Wiley, 1999

[12] KRAMER, D.: Status of BESSY II, a High Brilliance Synchrotron Light Source in the VUV to XUV Range. In: *Proceedings of the 1993 Particle Accelerator Conference* Vol. 2, May 17-20 1993, p. 1436–1438

[13] MILLS, D. M. et.al.: Report of the Working Group on Synchrotron Radation Nomenclature – brightness, spectral brightnes or brilliance? In: *J. Synchrotron Rad.* 12 (2005), p. 385

[14] PÜTTNER, Ralph: *Monochromatisierung von Synchrotronstrahlung*. Presentation Slides. Pictures courtesy of R. Follath.

[15] ROBINSON, Arthur L.: History of Synchrotron Radiation. In: *X-Ray Data Booklet*. Lawrence Berkeley National Laboratory, 2000. – URL http://xdb.lbl.gov/

[16] UNIVERSITÄT MAINZ: *Institut für Kernphysik*. Instituts-Prospekt. – URL http://www.kph.uni-mainz.de/information/introduction/

[17] WEISSTEIN, Eric: *Doppler Effect*. Online Resource: Eric Weisstein's World of Physics. – URL http://scienceworld.wolfram.com/physics/DopplerEffect.html

[18] WILLE, K.: Synchrotron Radiation Sources. In: *Rep. Prog. Phys.* 54 (1991), p. 1005–1068